State flip at exceptional points in atomic spectra

Henri Menke,* Marcel Klett,† Holger Cartarius, Jörg Main, and Günter Wunner
Institut für Theoretische Physik 1, Universität Stuttgart, 70550 Stuttgart, Germany
(Received 4 November 2015; published 4 January 2016)

We study the behavior of nonadiabatic population transfer between resonances at an exceptional point in the spectrum of the hydrogen atom. It is known that, when the exceptional point is encircled, the system always ends up in the same state, independent of the initial occupation within the two-dimensional subspace spanned by the states coalescing at the exceptional point. We verify this behavior for a realistic quantum system, *viz.*, the hydrogen atom in crossed electric and magnetic fields. It is also shown that the nonadiabatic hypothesis can be violated when resonances in the vicinity are taken into account. In addition, we study nonadiabatic population transfer in the case of a third-order exceptional point, in which three resonances are involved.

DOI: 10.1103/PhysRevA.93.013401

I. INTRODUCTION

In many cases a very effective way of investigating open quantum systems with a reasonable effort, in particular, to avoid expensive time-dependent calculations, is made possible by non-Hermitian Hamiltonians [1]. A typical example is resonances, i.e., decaying unbound states. With appropriate methods used as the complex scaling approach [1–5] resonances can be uncovered in a time-independent calculation as complex eigenvalues of the stationary Schrödinger equation. It is well known that resonances show characteristic effects not observable in Hermitian quantum systems. This is true, in particular, close to exceptional points (EPs) [1,6–8], isolated points in a physical parameter space, at which two or even more eigenstates coalesce.

The appearance of EPs has theoretically been shown in unstable lasers [9], optical waveguides [10], and resonators [11,12]. In quantum systems their existence has been proved in atomic [13–16] and molecular [17] spectra, in the scattering of particles at potential barriers [18], in atom waves [19–22], and in non-Hermitian Bose-Hubbard models [23]. Their relation to Fano resonances has been pointed out [24–26]. Experimental verification of their physical nature was achieved in microwave cavities [27–29], electronic circuits [30], metamaterials [31], a photonic crystal slab [32], and exciton-polariton resonances [33].

A simple example is the two-dimensional matrix

$$\boldsymbol{M}(\lambda) = \begin{pmatrix} 1 & \lambda \\ \lambda & -1 \end{pmatrix} \tag{1}$$

with a one-dimensional complex parameter λ. The eigenvalues are given by $\epsilon_1 = \sqrt{1+\lambda^2}$ and $\epsilon_2 = -\sqrt{1+\lambda^2}$. It is obvious that these eigenvalues share a common degeneracy for $\lambda = \pm i$ and the same holds for the eigenvectors; i.e., $\lambda = \lambda_c = \pm i$ is an EP. The example demonstrates one of the most striking features of an EP, which can be seen from a power-series expansion of the eigenvalues for a circle $\lambda(\varphi) = i + \varrho e^{i\varphi}$ with a small radius ϱ around an EP:

$$\epsilon_1 = \sqrt{2\varrho}e^{i(\pi/4+\varphi/2)}, \quad \epsilon_2 = \sqrt{2\varrho}e^{i(5\pi/4+\varphi/2)}. \tag{2}$$

Evidently the eigenvalues interchange their positions in energy space when the EP is encircled in a closed loop, i.e., $\varphi = 0 \ldots 2\pi$. Only after two circles do the eigenvalues return to their original positions, but the eigenvectors pick up a geometric phase, which is expressed by a sign change, e.g., $[\psi_1, \psi_2] \xrightarrow{\text{circle}} [\psi_2, -\psi_1]$.

This is an example of a second-order exceptional point (EP2), but higher-order EPs are also possible [6]. The simplest extension is a third-order exceptional point (EP3), at which three resonances coalesce, i.e., have identical eigenvalues and eigenvectors [20,21,34–37].

Uzdin *et al.* [38] as well as Berry and Uzdin [39] have shown that the adiabatic exchange of the states mentioned above will not be observable for the true temporal evolution of an occupied resonance state. Only one of the states behaves according to the adiabatic expectation. The reason is that nonadiabatic effects can never be neglected in the decay dynamics of resonances and the adiabatic connections [40] are no longer fulfilled. When an EP is encircled the occupation always ends up in the same state, independent of the initial occupation within the two-dimensional subspace of the resonances forming the EP [38,39,41–44]. Recently a careful analysis of the dynamics revealed that it is strongly nonintuitive [45]. Note that the adiabatic expectation with the exchange of two resonances can always be extracted from evaluations of their complex eigenvalues if the physical parameters are changed in small steps on a closed loop in the parameter space and the eigenvalues are then connected continuously, which has been shown in numerical studies and experiments [7,14,16,18,20,21,27–29,33].

It has been shown that EP2s can be exploited for the controlled occupation of a single quantum state [17,42,43]. However, in these considerations the two resonances coalescing at the EP have always been assumed to be isolated from all other states. This is very often not the case in physical systems. Leclerc *et al.* [46] have shown that the existence of further resonances in the vicinity of an EP can significantly influence the nonadiabatic temporal evolution and the exchange behavior of states at an EP.

In this paper we address this question in detail. We do this by investigating the resonances of the hydrogen atom in crossed electric and magnetic fields. It is especially suited for this investigation since numerically exact calculations of resonance states are feasible, a large number of EPs is

*Henri.Menke@itp1.uni-stuttgart.de
†Marcel.Klett@itp1.uni-stuttgart.de

known, and their properties are clearly observable [16,35,47]. In particular, examples of EPs with additional resonances in their neighborhood are available. Some possess neighboring resonances in their close vicinity; others are very isolated. In addition, a case of two adjacent EP2s has been discovered, where the permutation behavior of the resonances is exactly that of an EP3 if both EPs are encircled together. This gives us the opportunity to study nonadiabatic state transfer at EP3s.

The remaining sections of this article are organized as follows. In Sec. II we introduce our system, *viz.*, the hydrogen atom in crossed static electric and magnetic fields, the numerically accurate method to calculate the resonances of the system, and the evaluation of the temporal evolution of occupation probabilities of the resonances. The nonadiabatic evolution of the resonance states is then investigated in Sec. III for the case of an EP2 and an EP3. A discussion and conclusions are given in Sec. IV.

II. THE HYDROGEN ATOM IN CROSSED ELECTRIC AND MAGNETIC FIELDS

A. Resonances of the hydrogen atom

In atomic Hartree units without relativistic corrections or finite-nuclear-mass effects the Hamiltonian of the hydrogen atom in crossed static electric and magnetic fields reads

$$H = \frac{1}{2}\boldsymbol{p}^2 - \frac{1}{r} + \frac{1}{2}\gamma L_z + \frac{1}{8}\gamma^2(x^2+y^2) + fx, \qquad (3)$$

where L_z is the z component of the angular momentum, and $\gamma = B/B_0$ and $f = F/F_0$, with $B_0 = 2.35 \times 10^5$ T and $F_0 = 5.14 \times 10^9$ V/cm, are the dimensionless field strength parameters of the magnetic and electric fields, which are oriented along the z and x axis, respectively. The total energy and the parity with respect to the (x,y) plane are the constants of motion. The parity is the only remaining symmetry of the system and is exploited in the calculations. All subsequent studies are done in the symmetry subspace of states with even z parity. To calculate the resonances of the Hamiltonian the complex rotation method is applied [1–5]. By replacing the spacial coordinates $\boldsymbol{r}$ in the Hamiltonian and the wave functions with $b^2\boldsymbol{r}$, where b is a complex scaling parameter, we obtain a complex symmetric Hamiltonian, in which resonances appear as discrete complex energy eigenvalues. The real part of these complex eigenvalues represents the resonance energy; its imaginary part, the width.

With the introduction of semiparabolic coordinates a complex symmetric matrix representation of the Schrödinger equation can be set up in an oscillator basis [48]. This leads to the generalized eigenvalue problem

$$\boldsymbol{A}(\gamma,f)\phi = 2|b|^4 E\boldsymbol{C}\phi\ , \qquad (4)$$

where $\boldsymbol{A}(\gamma,f)$ is a complex symmetric matrix, $\boldsymbol{C}$ is a real symmetric positive definite metric, and E is the complex energy eigenvalue. The appropriate normalization of the eigenvectors in the complex extended system has to be done with the c-product [1] and reads, for the generalized eigenvalue problem, (4), $\phi_i \boldsymbol{C} \phi_j = \delta_{ij}$.

B. Temporal evolution of the occupation probabilities of the resonances

In our scheme the field strengths $\gamma(t)$ and $f(t)$ are varied time dependently such that closed loops are traversed in the parameter space. This results in a time-dependent matrix $\boldsymbol{A}(t)$ and, thus, also time-dependent resonance energies $E_i(t)$ and eigenstates $\phi_i(t)$. To study population transfer during the traversal of a closed loop around an EP we split the state by means of spectral decomposition into these time-dependent eigenstates $\phi_i(t)$ of the Hamiltonian; i.e., the expansion coefficients $a_i(t)$ define the occupation of a resonance state $\phi_i(t)$ which is an eigenstate of the Hamiltonian with the current field strengths $\gamma(t)$ and $f(t)$,

$$\psi(t) = \sum_i a_i(t)\phi_i(t). \qquad (5)$$

This corresponds to the instantaneous basis used in Ref. [38] to study nonadiabatic transfer in a matrix model. In the instantaneous basis the temporal evolution of the expansion coefficients following from the Schrödinger equation (4) reads

$$\dot{a}_i(t) = -iE(t)a_i(t) - \sum_j a_j(t)\phi_i(t)\boldsymbol{C}\dot{\phi}_j(t). \qquad (6)$$

The dominant effect is the decay of the resonances, which leads to a fast decrease in the occupation coefficients a_i.

For a better and more intuitive interpretation of the occupation transfer during a path around an EP we introduce weighted coefficients, for which the overall decay of the probability amplitude is removed. They are meant to illustrate the relative gain and loss. The weighted coefficients are denoted by an overbar and are given by

$$\bar{a}_i = |a_i|^2 \left(\sum_{j=1}^{N} |a_j|^2 \right)^{-1}, \qquad (7)$$

where N is the total number of states taken into account.

If there were no couplings between the eigenstates, i.e., $\phi_i \boldsymbol{C} \dot{\phi}_j = 0$, all populations would evolve independently and only the decay of the resonances with a time-dependent decay rate $\mathrm{Im}\,(E_i(t))$ would be observed. This adiabatic expectation can be formulated as

$$\dot{a}_{\mathrm{ad}}(t) = -iE(t)a_{\mathrm{ad}}(t). \qquad (8)$$

We use it to compare the full temporal evolution given by Eq. (6) with the adiabatic approximation.

III. STATE EXCHANGE FOR CIRCLES AROUND EXCEPTIONAL POINTS

A. Second-order exceptional point

In the following we study the population transfer at previously determined EPs [35]. First, we observe the behavior at a second-order EP, whose physical parameters are listed in the first row of data in Table I. To encircle the EP the parameters γ and f have to be varied in a specific way. They need to perform a closed loop; hence a good choice is a circle described by

$$\gamma(\varphi) = \gamma_0(1 + \delta\cos\varphi), \quad f(\varphi) = f_0(1 + \delta\sin\varphi), \qquad (9)$$

TABLE I. Coordinates of some exceptional points in the spectrum of the hydrogen atom in crossed magnetic (γ) and electric (f) fields. All values are given in atomic Hartree units.

γ	f	Re(E)	Im(E)
0.005388	0.0002619	−0.02360	−0.00015
0.00611	0.000256	−0.01593	−0.00024
0.00615	0.000265	−0.0158	−0.000374

where the pair (γ_0, f_0) represents the circle's center and δ is a radius chosen relative to the field strengths. The trajectories of the resonances in energy space for a relative radius $\delta = 10^{-2}$ are depicted in Fig. 1(a). The center was chosen exactly at the EP. The plot shows two resonances interchanging their positions during a traversal of the loop in the parameter space, which is shown in the inset. Two other resonances with a smaller modulus of the imaginary part are plotted alongside. There are even more resonances in the vicinity with greater moduli of the imaginary parts. Calculations also taking these into account were carried out, and it turned out that they do not influence the result.

We proceed to investigate how well the statement given by Uzdin *et al.* [38], *viz.*, that the final distribution of the populations is independent of the initial state, is visible in the case of the hydrogen atom with its large number of highly coupled states. Therefore we prepare the system with the full population starting in one of the two resonances belonging to the EP. In the first step we neglect all further states and, thus, effectively reduce the Hilbert space to two dimensions. In Fig. 2 the evolution is displayed. The line styles of the respective coefficients a_i (excluding a_{ad}, of course) correspond to those shown in the map in Fig. 1. We find that the adiabatic

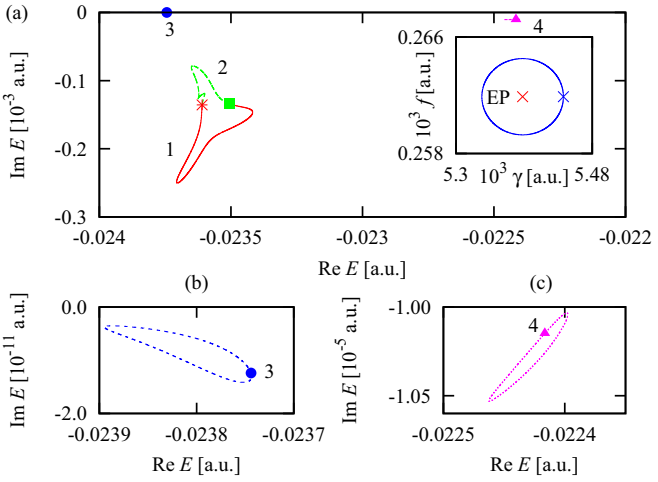

FIG. 1. (a) Two resonances interchanging their positions in the complex energy plane for a parameter-space circle (inset) around the exceptional point listed in the first row of data in Table I. The center of the parameter-space circle is identical to the exceptional point and $\delta = 10^{-2}$ was chosen. The initial point in the parameter plane and the corresponding energy values of the resonances are represented by symbols on the lines. (b, c) Dynamics of two nearby resonances with small imaginary parts, which are visible only as filled symbols in (a) and are marked by the labels 3 and 4.

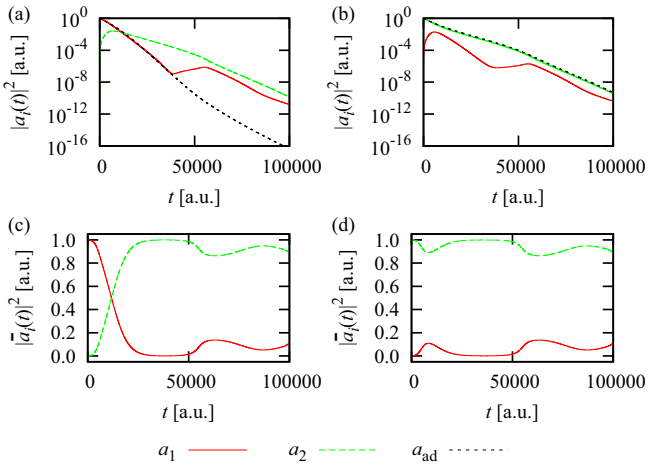

FIG. 2. Temporal evolution of the populations. Only the two resonances connected with the exceptional point were taken into account. (a, b) The actual populations are plotted for an initial population $a_1(0) = 1$ and $a_2(0) = 1$, respectively. The overall evolution is dominated by the decay emergent from the nonzero imaginary parts of the eigenvalues. (c) and (d) Weighted coefficients according to Eq. (7) are shown (c) for the initial condition of (a) and (d) for the initial condition of (b). Results of the adiabatic approximation (a_{ad}) are shown for comparison.

hypothesis is perfectly met for the case of the population being fully prepared in a_2, which can be graphically verified in Fig. 2(b). The final state is, in both cases, a majority population of the state labeled a_2 and a minority of that identified as a_1.

However, this behavior changes completely if we take into account the resonances with smaller moduli of the imaginary parts in the vicinity of the two states. An example is depicted in Fig. 3, where all four resonances shown in Fig. 1 have been used for the calculation of the temporal evolution. Due to nonadiabatic couplings among all four resonances the states represented by a_3 and a_4 gain in population even though no population was initially prepared in them. It is even more surprising that resonance a_4 dominates in the end. In principle, one would expect the majority to end up in the resonance a_3, as this is a nearly bound state with the lowest imaginary part. This is indeed what is going to happen, but not on the time scales we used in the calculations. Since the time is not sufficient for the occupation in a_4 to vanish, the stronger coupling of that state to a_1 and a_2 determines the final population. The important statement holds in spite of this, *viz.*, that the populations of the states performing the exchange vanish, while the populations of the states with small imaginary parts persist.

B. Importance of exceptional points for the exchange behavior

We have seen that the decay rates, i.e., the imaginary parts of the complex energy eigenvalues, basically determine which nearby resonance of an initially occupied state survives at the end of the parameter-space loop. This raises the question whether the EP really is important for the exchange behavior since nonadiabatic couplings and strongly unequal decay rates can appear without the existence of EPs for any pair of resonances with similar energies as well. To address this question we move the center of the parameter-space circle

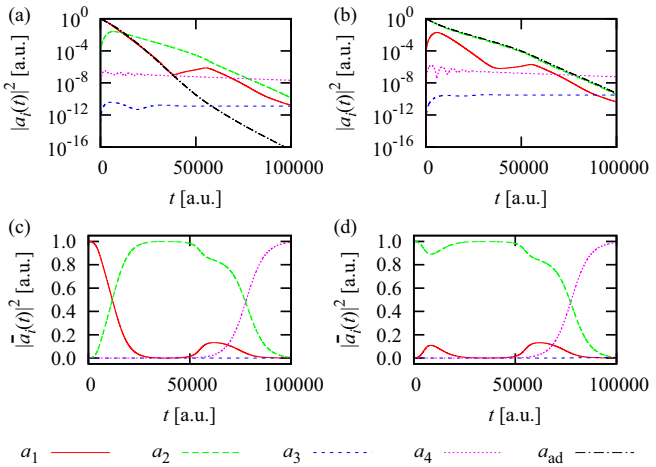

FIG. 3. Temporal evolution of the populations with all four resonances taken into account. (a) The initial population was exclusively in the resonance described by the coefficient a_1; (b) only a_2 was initially populated. In (a) and (b) it is already visible that the resonances with smaller moduli of the imaginary parts decay much more slowly. Eventually the resonance with a smaller modulus of the imaginary part dominates. (c, d) This is especially clearly visiblehere, where the weighted coefficients for the cases in (a) and (b), respectively, are shown. The whole surviving population transfers into the resonance represented by a_4.

as shown in Fig. 4(a). The first circle is, as before, exactly centered at the EP. Then it is shifted in small steps to larger values of γ via the shift parameter s. The modified circle reads

$$\gamma(\varphi) = \gamma_0[1 + \delta(s + \cos\varphi)], \quad f(\varphi) = f_0(1 + \delta \sin\varphi). \tag{10}$$

To get an intuitive insight we reduce the calculation, again, to the two resonances involved in the EP. This removes the overall effect of the unavoidable transition to the slowest decaying nearby resonance and helps us to focus on the effect of the EP.

The temporal evolution of the resonances in this case is shown in Fig. 4(b), and the representation with weighted coefficients in Fig. 4(c). In all cases the initial population was exclusively in the state labeled with the coefficient a_1. This is the nonadiabatic case from above. As long as the EP is located inside the parameter-space loop there are only slight changes in the temporal evolution. In particular, the final majority population of coefficient a_2 remains unchanged. As soon as the EP lies outside the parameter-space circle the evolution of the occupations changes suddenly. One can observe that for $s = 1.1$ the dominating population is in the coefficient a_1, a result which agrees with the adiabatic expectation. Since there is no longer a permutation of the resonances even in the purely adiabatic case if the EP is not encircled, the switch of the majority population from one state to the other is not very surprising. However, the influence of the EP is even stronger. It is additionally expressed in the total difference of the occupation of both states. If an EP is encircled, it is much more pronounced as in the case in which there is no EP within the circle.

For an even stronger shift of the circle the difference in the final populations of a_1 and a_2 is reduced further and the

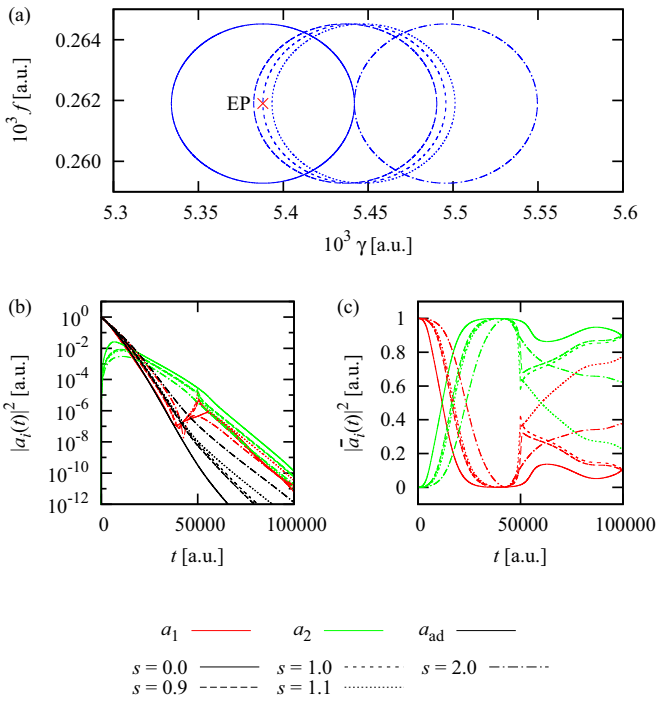

FIG. 4. The center of the circle in parameter space is shifted in the positive γ direction to study the transition from an interchange scenario to a noninterchange case. (a) Circles for different values of s as introduced in Eq. (10). The time evolution of the absolute (b) and weighted (c) coefficients demonstrate a significant qualitative change as soon as the exceptional point is no longer located within the parameter-space loop. The line styles of the circles correspond to those used in the temporal evolution. For nonweighted coefficients the adiabatic expectation is plotted alongside.

majority population switches again. This happens in a smooth way and can be traced back to the different decay rates.

The whole scenario can be understood even better by viewing Fig. 5, in which the final population of both resonances is shown in dependence on the shift parameter s. The dramatic influence of the EP becomes immediately clear due to the sudden jump of both populations at the value $s = 1$, for which the parameter-space circle crosses the EP. Thus, the total behavior revealed in Figs. 2 and 3 cannot be explained by

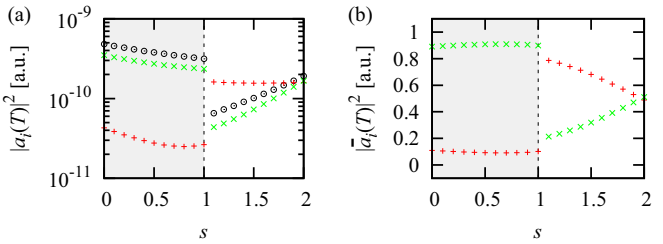

FIG. 5. Final values of the coefficients after a full traversal of the circle in parameter space as a function of the shift parameter s, where the absolute coefficients (a) and their weighted counterparts (b) are shown. The (red) plus symbols represent a_1; (green) X's, a_2; and black circles, the adiabatic approximation. The shaded area (left half) denotes that the circle for this value of s encircles the exceptional point.

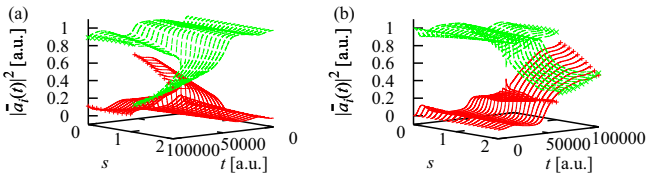

FIG. 6. Weighted coefficients $|a_i|^2$ from Fig. 5 as a function of the shift parameter s and the evolved time t. (a, b) Two views of the (s,t) plane. One clearly recognizes the dramatic change as soon as the exceptional point is within the parameter-space circle, indicating the switch from one Riemann surface to the other.

the nonadiabatic couplings and the different decay rates alone. The presence of the EP is essential.

The relevance of the EP also becomes clear in Fig. 6, in which the two weighted coefficients are plotted in dependence of the shift parameter s and the evolved time t. It is shown that those paths which encircle the EP lead to a dramatic change in the occupation probabilities. For values $s \gtrapprox 1$, i.e., close to the EP, the switch from one Riemann surface to the other becomes observable. However, for larger shifts, $s \approx 2$, nonadiabatic processes lead to a change in the final result.

C. Third-order exceptional point

The hydrogen atom does not possess just EP2s. A structure identical to that of an EP3 has also been detected [16]. It is uncovered by encircling the two EPs in the last two rows of data in Table I simultaneously. An energy map of the resulting scheme of interchange is depicted in Fig. 7 for $\gamma_0 = 0.00609$, $f_0 = 0.000261$, and a radius $\delta = 3.0 \times 10^{-2}$. One can see that all three resonances are permuted. In this case a closed loop of a single resonance in the complex energy plane is only achieved by three circles in the parameter space.

As in the case of the EP2 we first perform calculations which take into account only the three resonances connected to the EP3 structure. This allows us to study the nonadiabatic temporal evolution of an unperturbed EP3. For each

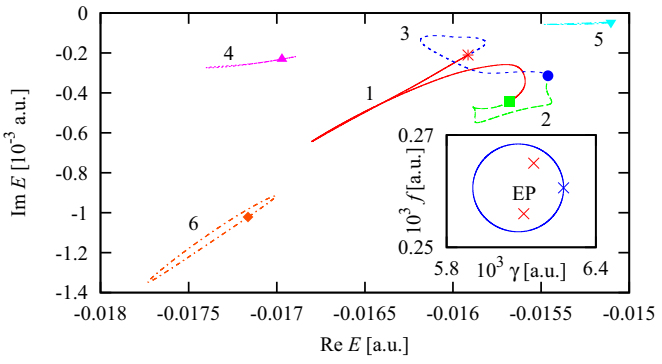

FIG. 7. Map of the energy space of a structure identical to that of a third-order exceptional point for a parameter-space circle around the two exceptional points from the last two rows of data in Table I (see inset). The plot shows three resonances interchanging their positions and some nearby resonances in the energy space. Energy eigenvalues for the initial point in the parameter-space circle are represented by symbols on the lines.

calculation we prepare the initial population fully in one of these states. The results are plotted in Fig. 8. To facilitate the comparison the line styles correspond to those in the map in Fig. 7. Figures 8(a) and 8(d) correspond to the system being initially prepared in the state a_1. Until about halfway through the circle in parameter space the system evolves adiabatically as shown in Fig. 8(a); i.e., the line of a_1 is exactly on top of that for the adiabatic case. However, then the lines separate and the state associated with a_3 exceeds the a_1 curve in amplitude. Figure 8(d) shows essentially the same situation, but for the coefficients weighted according to Eq. (7). Here we see that the population of the state associated with a_1 is transferred to the state associated with a_3, whereas the state with a_2 is not involved in the population transfer at all.

Figures 8(b) and 8(e) depict the situation for the initial population being prepared in a_2. Even though there is some transition to a_1 at first, the coefficient a_3 soon dominates. After a_3 ascends to the population leader, a_2 no longer contributes to the population. If the system is prepared with the initial population in a_3 it evolves adiabatically until the end of the present cycle time [cf. Figs. 8(c) and 8(f)]. As observed above for the other cases the system also starts off adiabatically but eventually deviates from this behavior. Hence for the initial population in a_1 or a_2 a state flip occurs. This is particularly visible in the weighted coefficients in Figs. 8(c)–8(f). With these results we can extend the statement given by Uzdin *et al.* [38] to the scenario of three permuting resonances. Also in this case the final distribution of the populations is independent of the initial state. In the example considered it always ends up in a_3.

Of course, the three resonances forming the EP3 are not isolated in the spectra of the hydrogen atom as we observed for the EP2. Here the closest three resonances have to be taken into account to obtain a realistic temporal evolution. All of them are included in Fig. 7. Considering the imaginary parts of the resonances during the whole parameter-space loop we have one that is strictly larger, one that is strictly smaller, and one that lies somewhere in between those of the interchanging resonances. The time evolution is depicted in Fig. 9 in the same way as in Fig. 8.

Starting from the left Fig. 9(a) corresponds to the initial population being prepared fully in the state represented by a_1. Here, the system evolves adiabatically at first, but eventually a_5 exceeds all others in terms of magnitude. This is even more visible in the plot for the weighted coefficients shown in Fig. 9(d), where a_5 rapidly approaches unity after about a quarter of the traversal time and then does not change for the rest of the evolution. A similar behavior is observed for an initial population of only the state represented by a_2, though a_5 approaches unity even faster in the weighted representation shown in Fig. 9(e). While the population prepared fully in the state corresponding to a_3 evolved adiabatically when nearby resonances were neglected, we again observe a transition to a_5 in the extended case as shown in Figs. 9(c) and 9(f).

We conjecture that the transition from all other resonances to a_5 is induced by nonadiabatic couplings. This is certainly an effect of the close distance between the resonance of a_5 and the interchanging resonances in energy space (cf. Fig. 7). One could now claim that the other resonances taken into account are also at a close distance and should acquire a considerable

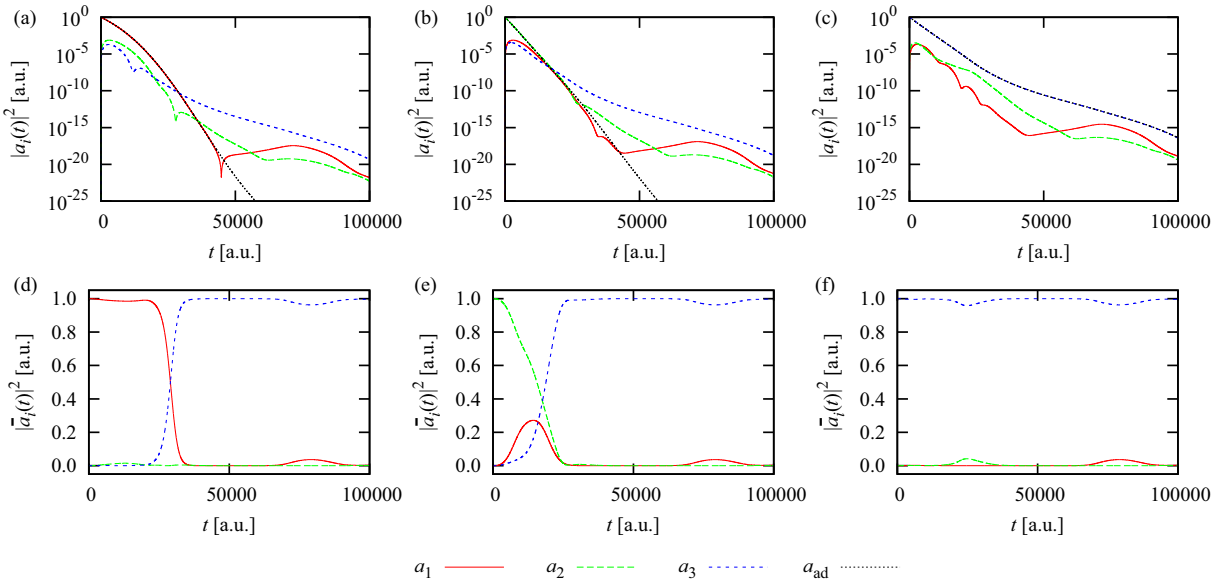

FIG. 8. Temporal evolution of the populations for a circle around a third-order exceptional point. Initial populations were set up in (a, d) a_1, (b, e) a_2, and (c, f) a_3. In the case of the initial population being prepared in a_3 the system evolves adiabatically. In all cases the nondissipated population ends up in a_3. This is clearly shown by the weighted coefficients $\bar{a}_i$.

occupation during the traversal of the loop. However, this is not the case. They are even invisible in the diagram of the weighted coefficients. This happens because their imaginary parts are substantially larger than that of the resonance belonging to a_5, which results in a faster decay of their population.

IV. DISCUSSION AND CONCLUSIONS

In summary, we were able to show that the nonadiabatic state flip at an EP2 is also observable in the temporal evolution of occupied resonances of the hydrogen atom in crossed electric and magnetic fields. If only the two resonances connected to an EP are taken into account, the system always ends up in the same state independent of the initial condition as in all previous studies [38,39,42–46] if a parameter-space loop around the EP is performed. However, the spectra of the hydrogen atom always exhibit further resonances in the vicinity of those forming the EP, which can drastically influence the final occupation [46]. A coupling to these states cannot be neglected and eventually the state with the lowest decay rate dominates. This was verified in numerically exact calculations for the hydrogen atom.

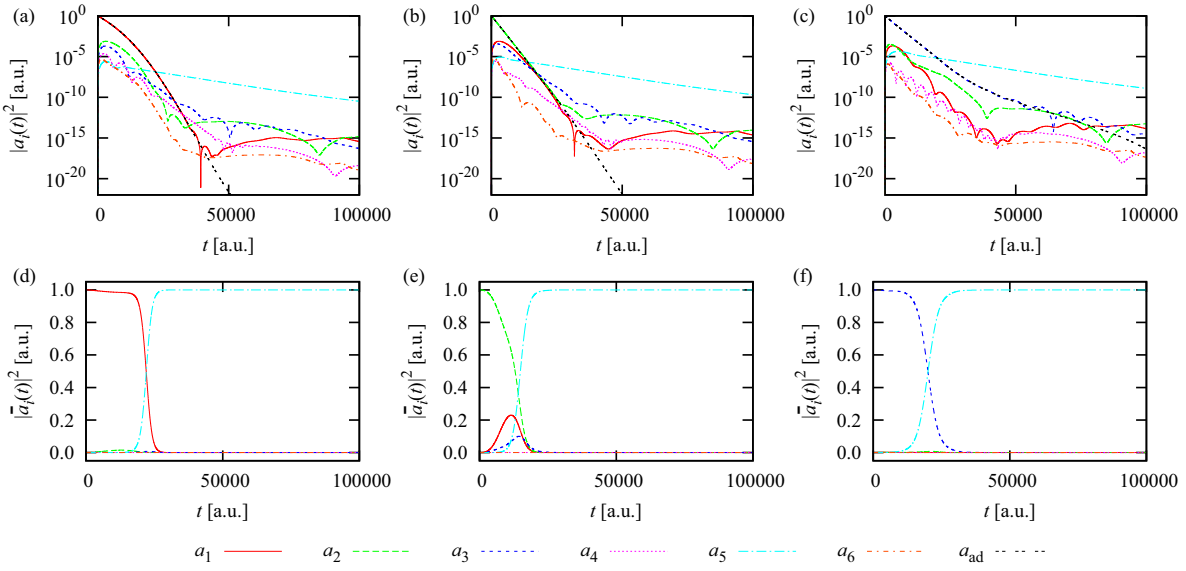

FIG. 9. Temporal evolution of the populations for the same parameter-space circle as in Fig. 8 but with six resonances taken into account in the calculation. Again, initial populations were set up in (a, d) a_1, (b, e) a_2, and (c, f) a_3. The population always ends up in the resonance with the least modulus of the imaginary part, here a_5.

Even though the nonadiabatic couplings in combination with different decay rates basically determine which resonance is occupied after the traversal of a parameter-space loop, they are not the only relevant information. The temporal evolution is strongly influenced by the presence of an EP. If it is located within the parameter-space loop, the difference in the final occupation is exchanged and increases drastically.

Similar relations hold for EP3s. If couplings to further resonances can be neglected and the traversal time is long enough, the final population always ends up in the same state and does not depend on the initial population of the three states forming the EP3. As in the EP2 case for a realistic scenario in an atomic system further resonances have to be considered and lead to a change in the behavior in favor of the exclusive population of a nearby resonance in energy space with the lowest decay rate.

The calculations reported in this work clearly show that the observation of the characteristic nonadiabatic population transfer at EPs will only be possible if sufficiently isolated resonances are accessible. In an atomic or molecular quantum system this will be a big challenge. For the hydrogen atom we have to remark that the parameter range we used in the calculations was chosen due to the numerical capabilities and includes a basis with approximately 10 000 states. This makes accessible relatively low-lying energies which have to be influenced by strong fields (magnetic field $\approx$1000 T, electric field $\approx 10^6$ V/cm), resulting in short decay times. Even though extremely low surviving probabilities were accepted in the calculations the traversal time of the parameter-space loop is of the order of 10^{-11} s. In an experiment this could be overcome by aiming at resonances states at higher energies, which additionally increases the probability of the appearance of EPs since the density of states is higher, or by investigating an almost-equivalent system. Hydrogen-like excitons in semiconductor structures would lower the physical parameters to accessible values and could be studied in experiments [49].

[1] N. Moiseyev, *Non-Hermitian Quantum Mechanics* (Cambridge University Press, Cambridge, UK, 2011).
[2] W. P. Reinhardt, Annu. Rev. Phys. Chem. **33**, 223 (1982).
[3] N. Moiseyev, Phys. Rep. **302**, 212 (1998).
[4] D. Delande, A. Bommier, and J. C. Gay, Phys. Rev. Lett. **66**, 141 (1991).
[5] Y. Ho, Phys. Rep. **99**, 1 (1983).
[6] W. D. Heiss, J. Phys. A **45**, 444016 (2012).
[7] W. D. Heiss, Eur. Phys. J. D **7**, 1 (1999).
[8] T. Kato, *Perturbation Theory for Linear Operators* (Springer, New York, 1966).
[9] M. V. Berry, J. Mod. Opt. **50**, 63 (2003).
[10] S. Klaiman, U. Günther, and N. Moiseyev, Phys. Rev. Lett. **101**, 080402 (2008).
[11] J. Wiersig, S. W. Kim, and M. Hentschel, Phys. Rev. A **78**, 053809 (2008).
[12] J. Wiersig, Phys. Rev. Lett. **112**, 203901 (2014).
[13] A. I. Magunov, I. Rotter, and S. I. Strakhova, J. Phys. B **32**, 1489 (1999).
[14] A. I. Magunov, I. Rotter, and S. I. Strakhova, J. Phys. B **34**, 29 (2001).
[15] O. Latinne, N. J. Kylstra, M. Dörr, J. Purvis, M. Terao-Dunseath, C. J. Joachain, P. G. Burke, and C. J. Noble, Phys. Rev. Lett. **74**, 46 (1995).
[16] H. Cartarius, J. Main, and G. Wunner, Phys. Rev. Lett. **99**, 173003 (2007).
[17] R. Lefebvre, O. Atabek, M. Šindelka, and N. Moiseyev, Phys. Rev. Lett. **103**, 123003 (2009).
[18] E. Hernández, A. Jáuregui, and A. Mondragán, J. Phys. A **39**, 10087 (2006).
[19] K. Rapedius, C. Elsen, D. Witthaut, S. Wimberger, and H. J. Korsch, Phys. Rev. A **82**, 063601 (2010).
[20] H. Cartarius, J. Main, and G. Wunner, Phys. Rev. A **77**, 013618 (2008).
[21] R. Gutöhrlein, J. Main, H. Cartarius, and G. Wunner, J. Phys. A **46**, 305001 (2013).
[22] N. Abt, H. Cartarius, and G. Wunner, Int. J. Theor. Phys. **54**, 4054 (2015).
[23] E. M. Graefe, U. Günther, H. J. Korsch, and A. E. Niederle, J. Phys. A **41**, 255206 (2008).
[24] A. I. Magunov, I. Rotter, and S. I. Strakhova, Phys. Rev. B **68**, 245305 (2003).
[25] W. D. Heiss and G. Wunner, Eur. Phys. J. D **68**, 284 (2014).
[26] L. Schwarz, H. Cartarius, G. Wunner, W. D. Heiss, and J. Main, Eur. Phys. J. D **69**, 196 (2015).
[27] C. Dembowski, H.-D. Gräf, H. L. Harney, A. Heine, W. D. Heiss, H. Rehfeld, and A. Richter, Phys. Rev. Lett. **86**, 787 (2001).
[28] B. Dietz, H. L. Harney, O. N. Kirillov, M. Miski-Oglu, A. Richter, and F. Schäfer, Phys. Rev. Lett. **106**, 150403 (2011).
[29] S. Bittner, B. Dietz, H. L. Harney, M. Miski-Oglu, A. Richter, and F. Schäfer, Phys. Rev. E **89**, 032909 (2014).
[30] T. Stehmann, W. D. Heiss, and F. G. Scholtz, J. Phys. A **37**, 7813 (2004).
[31] M. Lawrence, N. Xu, X. Zhang, L. Cong, J. Han, W. Zhang, and S. Zhang, Phys. Rev. Lett. **113**, 093901 (2014).
[32] B. Zhen, C. W. Hsu, Y. Igarashi, L. Lu, I. Kaminer, A. Pick, S.-L. Chua, J. D. Joannopoulos, and M. Soljacic, Nature **525**, 354 (2015).
[33] T. Gao, E. Estrecho, K. Y. Bliokh, T. C. H. Liew, M. D. Fraser, S. Brodbeck, M. Kamp, C. Schneider, S. Höfling, Y. Yamamoto, F. Nori, Y. S. Kivshar, A. G. Truscott, R. G. Dall, and E. A. Ostrovskaya, Nature **526**, 554 (2015).
[34] W. D. Heiss, J. Phys. A **41**, 244010 (2008).
[35] H. Cartarius, J. Main, and G. Wunner, Phys. Rev. A **79**, 053408 (2009).
[36] G. Demange and E.-M. Graefe, J. Phys. A **45**, 025303 (2012).
[37] H. Eleuch and I. Rotter, Eur. Phys. J. D **69**, 230 (2015).
[38] R. Uzdin, A. Mailybaev, and N. Moiseyev, J. Phys. A **44**, 435302 (2011).
[39] M. V. Berry and R. Uzdin, J. Phys. A **44**, 435303 (2011).
[40] V. Arnold, Sel. Math. **1**, 1 (1995).
[41] I. Gilary and N. Moiseyev, J. Phys. B **45**, 051002 (2012).

[42] I. Gilary, A. A. Mailybaev, and N. Moiseyev, Phys. Rev. A **88**, 010102 (2013).
[43] E.-M. Graefe, A. A. Mailybaev, and N. Moiseyev, Phys. Rev. A **88**, 033842 (2013).
[44] D. Viennot, J. Phys. A **47**, 065302 (2014).
[45] T. J. Milburn, J. Doppler, C. A. Holmes, S. Portolan, S. Rotter, and P. Rabl, Phys. Rev. A **92**, 052124 (2015).
[46] A. Leclerc, G. Jolicard, and J. P. Killingbeck, J. Phys. B **46**, 145503 (2013).
[47] H. Cartarius and N. Moiseyev, Phys. Rev. A **84**, 013419 (2011).
[48] J. Main and G. Wunner, J. Phys. B **27**, 2835 (1994).
[49] T. Kazimierczuk, D. Fröhlich, S. Scheel, H. Stolz, and M. Bayer, Nature **514**, 343 (2014).